Металлофиз. новейшие технол. / *Metallofiz. Noveishie Tekhnol.*
2016, т. 38, № 2, сс. 189–203 / DOI: 10.15407/mfint.38.02.0189
Оттиски доступны непосредственно от издателя
Фотокопирование разрешено только
в соответствии с лицензией

ФИЗИКА ПРОЧНОСТИ И ПЛАСТИЧНОСТИ

PACS numbers: 62.20.fg, 62.20.me, 62.25.Fg, 62.25.Mn, 81.40.Jj, 81.40.Np, 81.70.Cv

High Frequency Vibrations Impact on Mechanical Properties of Nanocrystalline Titanium

S. A. Bakai, R. V. Smolianets*, K. V. Kovtun, V. A. Moskalenko*, and A. S. Bakai

National Scientific Center 'KIPT', N.A.S. of Ukraine,
1 Akademichna Str.,
61108 Kharkiv, Ukraine
**B. I. Verkin Institute for Low Temperature Physics and Engineering of the National Academy of Sciences of Ukraine,*
47 Nauky Ave.,
61103 Kharkiv, Ukraine

Mechanical properties of nanocrystalline titanium are studied under uniform confined compression with ultrasound oscillations of 20 kHz to clarify the way of high-frequency vibrations' effect on mechanical properties of nanocrystals. The nanocrystalline VT1-0 titanium of commercial purity used in the experiments is fabricated employing cryogenic grain-fragmentation technique. This material has a broad distribution in grain size (20–80 nm) with the average size amounting to 40 nm. The amplitude of cyclic stress approaches 275 MPa. The high-frequency vibrations are found to lower the yield stress and to initiate the formation of shear bands. With the deformation rate of 10^{-4} s^{-1}, the yield stress becomes 2.5 times lower, and the major shear band forms under the deformation of 0.11 that is 5.7 times lower than the true deformation before the major shear band formation without action of the vibrations. On increasing the deformation rate up to 10^{-3} s^{-1}, the consequences of high-frequency vibrations' impact are weaken substantially.

Key words: nanoscale titanium, mechanical properties, strength, ductility, high-frequency vibrations.

Для з'ясування питання про вплив високочастотних вібрацій на механіч-

Corresponding author: Sergey Alexandrovich Bakai
E-mail: serg.bakai@kipt.kharkov.ua

Please cite this article as: S. A. Bakai, R. V. Smolianets, K. V. Kovtun, V. A. Moskalenko, and A. S. Bakai, High Frequency Vibrations Impact on Mechanical Properties of Nanocrystalline Titanium, *Metallofiz. Noveishie Tekhnol.*, **38**, No. 2: 189–203 (2016), DOI: 10.15407/mfint.38.02.0189.

ні властивості нанокристалів виконано дослідження механічних властивостей нанокристалічного титану при однорідному тривісному стисканні під дією ультразвукових коливань із частотою у 20 кГц. Використаний в експериментах нанокристалічний титан промислової чистоти ВТ1-0 одержано методом кріогенної фраґментації зерен. Цей матеріял має широкий розподіл зерен за розмірами (20–80 нм) із середнім розміром біля 40 нм. Амплітуда циклічних напружень сягала 275 МПа. Встановлено, що високочастотні вібрації знижують поріг пластичности й ініціюють утворення катастрофічних смуг зсуву. За швидкости деформації у 10^{-4} $с^{-1}$ поріг пластичности під дією вібрацій знижується в 2,5 рази, а катастрофічна смуга зсуву утворюється при деформації 0,11, яка є у 5,7 разів нижчою, ніж істинна деформація до моменту утворення катастрофічної смуги зсуву без дії вібрацій. При збільшенні швидкости деформації до 10^{-3} $с^{-1}$ ефекти дії високочастотних вібрацій істотно послаблюються.

Ключові слова: наномасштабний титан, механічні властивості, міцність, пластичність, високочастотна вібрація.

Для выяснения вопроса о влиянии высокочастотных вибраций на механические свойства нанокристаллов выполнены исследования механических свойств нанокристаллического титана при однородном трёхосном сжатии под действием ультразвуковых колебаний с частотой 20 кГц. Использованный в экспериментах нанокристаллический титан промышленной чистоты ВТ1-0 получен методом криогенной фрагментации зёрен. Этот материал имеет широкое распределение зёрен по размерам (20–80 нм) со средним размером, равным 40 нм. Амплитуда циклических напряжений достигала 275 МПа. Установлено, что высокочастотные вибрации снижают порог пластичности и инициируют образование катастрофических полос сдвига. При скорости деформации 10^{-4} $с^{-1}$ порог пластичности под действием вибраций снижается в 2,5 раза, а катастрофическая полоса сдвига образуется при деформации 0,11, которая в 5,7 раза ниже, чем истинная деформация до момента образования катастрофической полосы сдвига без воздействия вибраций. При увеличении скорости деформации до 10^{-3} $с^{-1}$ эффекты воздействия высокочастотных вибраций существенно ослабляются.

Ключевые слова: наномасштабный титан, механические свойства, прочность, пластичность, высокочастотная вибрация.

(Received December 7, 2015)

1. INTRODUCTION

Nanocrystalline metallic materials with submicron grain structure have promising mechanical properties. Their enhanced strength (compared to that of large-grain polycrystals) combines with sufficient yield, high resistance to wear, fatigue and corrosion (see, *e.g.*, [1–10]). Besides, nanocrystalline titanium and titanium-based alloys also have a relatively low specific weight and high corrosion stability. Due to a

combination of such properties, this material finds application in health care [11] and various high technology devices.

A large number of papers are devoted to the research into mechanical properties of nanocrystalline titanium (see [12–18] and the references therein). The material applicability domain depends also on the sensitivity of its mechanical characteristics to the impact of vibrations generating cyclic stresses. In combination with quasi-static stresses, the vibrations lead to irreversible structure changes and fatigue degradation of mechanical properties. Therefore, studying the impact of cyclic stresses on mechanical properties of nanocrystalline titanium is required to reveal the opportunity of its application in the presence of vibrations.

Fatigue tests of the coarse-grained titanium of commercial purity under low frequency (100 Hz) and high frequency (20 kHz) cyclic loading demonstrated that the high-cyclic (number of cycles amounting to $N \sim 10^8$) fatigue endurance limit comprised about $\cong 60\%$ of the yield stress under low-frequency as well as high-frequency tests. Weak sensitivity of coarse-grained titanium fatigue to the cyclic stress rate is attributed to the irreversible evolution of the dislocation structure playing the main role in fatigue processes in this material and resulting finally in the fatigue crack formation [19, 20]. Along with that, it is revealed that the more brittle, crystallographic and intergranular mode of the catastrophic crack formation takes place at the high frequency loading.

Papers [5, 14] outline the data of low-frequency fatigue tests of fine-grain titanium (submicron grain size), which, as demonstrated, differ substantially from similar data obtained under study of coarse-grain titanium. This difference is associated with shear restructuring in boundary layers which role grows with the density boundary increase.

Wide spectrum of boundary structure relaxation rates and the local heating of boundaries under shear restructuring induced by cyclic stresses lead to a substantial dependence of dynamic structure changes on cycling frequency in boundary layers. Therefore, one has no ground to assume that the impact of high-frequency and low-frequency cyclic stresses on mechanical properties of nanocrystalline metals and coarse-grain polycrystals will be identical [19, 20].

On decreasing the average grain size (d) the concentration of dislocation pinning centres also increases, $\propto a/d$ (a is the average interatomic distance), and the density of the grain boundaries grows in the same proportion as well, $\propto 1/d$. The contribution of extensive two-dimensional defects impeding dislocation slipping (grain boundaries, dislocation walls, declinations) into the yield stress is expressed with the Hall–Petch relation:

$$\sigma_{0.2} = \sigma_{0.2}^{\infty} + Kd^{-1/2}. \qquad (1)$$

Here, $\sigma_{0.2}$ is the yield stress; $\sigma_{0.2}^{\infty}$ is the yield stress of the crystal with a low concentration of two-dimensional extensive defects; d is the average distance between two-dimensional defects impeding dislocation slipping; K is the empiric proportionality factor. Grain boundaries are the main two-dimensional defects in a nanocrystalline metal. Therefore, conventionally, d is assumed in formula (1) to be equal to the average grain size. On one hand, dislocation pinning by grain boundaries makes a material more durable. On the other hand, boundary density growth increases the contribution of shear boundary restructuring (slipping) and cooperative processes initiated by this restructuring into the plastic deformation [1, 2]. Vibrations' impact on structure evolution and shear displacements in boundary layers produces changes in durability, in plastic deformation modes and failure of a nanocrystalline material.

Recent experimental studies into the grain-size dependence of various cooperative mechanisms of plastic deformation under uniaxial loading [21] permitted to establish the existence of critical grain size, $d_c \approx 15$ nm, below which the dislocation mechanism of plastic deformation does not play a substantial role, and the plasticity is provided by the cooperative rotational motion and dislocation-free boundary grain slipping (this result was obtained earlier by numerical modelling [22]). The theory of the strength and dislocation-free slipping in layers with random microscopic potential relief created for describing mechanical properties of metallic glasses [23–25] is also applicable to nanocrystalline metals when the dislocation plasticity mechanism is suppressed. Papers [21] and [24, 25] discuss a similarity between mechanical properties of nanocrystalline metals at $d < d_c$ and metallic glasses possessing a polycluster structure with the cluster size of $\cong 10$ nm. Research reported in papers [26, 27] reveals a high fatigue sensitivity of metallic glasses to ultrasonic oscillations permitting to expect substantial effects of high frequency vibrations impact on mechanical properties of nanocrystalline metals.

The studies which results are reported in the present communication were aimed at discovering the manifestations of the impact caused by high frequency vibrations of the ultrasound range ($\cong 20$ kHz) on mechanical properties of nanocrystalline titanium (with grain size below 100 nm) under uniaxial confined compression.

2. MATERIAL UNDER STUDY AND EXPERIMENTAL TECHNIQUE

In experiments, we employed the samples of nanocrystalline α-titanium of commercial purity VT1-0 produced by cryomechanical grain fragmentation (CMGF) of coarse grain material [16–18]. The CMGF technique consists in multiple rolling of the initial coarse-grain metal at liquid nitrogen temperature. The CMGF technique allows to

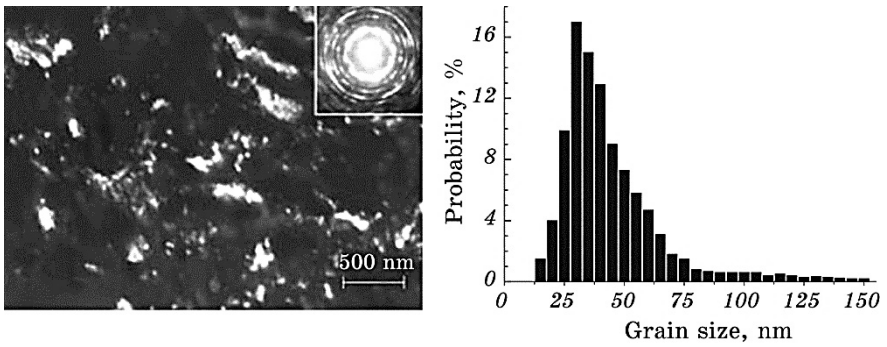

Fig. 1. Dark-field TEM image with the microelectronogram (*a*); grain size distribution histogram (*b*).

prepare ultra-fine grained metals with the grain size below 100 nm in contrast to other ones using intense plastic deformation for the titanium grain size decrease (as well as for other metals possessing the hexagonal densely packed lattice) and permitting conventionally to achieve the values exceeding 100 nm [5].

In order to prepare the samples used in the experiments, we employed nanocrystalline titanium produced in the form of slabs 3 mm thick through cryogenic rolling of large-grain material. The actual slab deformation value equals $e_{th} = 1.6$. Figure 1 presents the dark-field image of the structure produced with transmission electron microscopy (TEM) and the histogram of the grain size distribution. The average grain size is $\langle d \rangle \cong 40$ nm.

Cylindrical samples of 2.52 mm in diameter and 4 mm in height were cut at the VR-95d spark-cutting device. The deviation angle between the sample axis and its base from 90° does not exceed 20′. Taking into account the grain texture changes during cryogenic rolling, we prepared two sets of samples cut along and across the rolling direction, as is shown in Fig. 2.

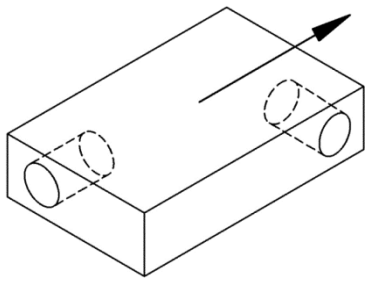

Fig. 2. Schematic cutting of specimens for mechanical testing in compression.

The samples belonging to different sets have a bit different Young's modulus and yield stress values, but we did not reveal substantial qualitative differences in the behaviour of both sets under the ultrasonic waves' action. In this communication, we present the data of mechanical testing samples from set 1 cut along the axis of rolling.

The Young's modulus of the nanocrystalline titanium under study was about 107 GPa at room temperature that was less than one for coarse-grain titanium (114–115 GPa). The yield stress, $\sigma_{0.2}$, approached the values about 850 MPa that approximately three times exceeded the yield stress of the coarse-grain VT1-0 titanium. Mechanical tests are performed at a specially designed bench [28] where samples may be uniformly loaded with simultaneous action of high frequency cyclic stresses. Figure 3 presents the bench setup.

The installation is intended for performing research into mechanical properties of materials in the presence or absence of ultrasonic vibrations under following conditions:

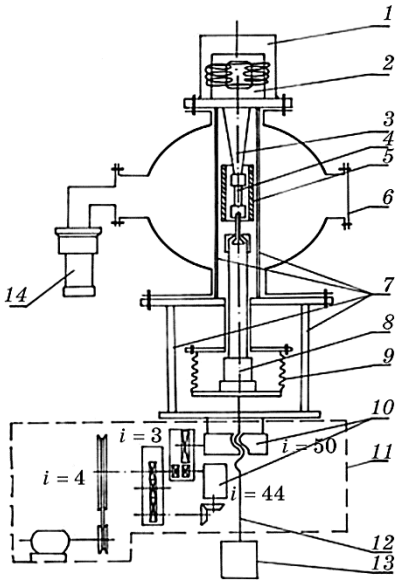

Fig. 3. Scheme of the installation for studying the ultrasonic vibrations impact on mechanical properties of materials in a broad temperature and deformation rate ranges. In the figure, we make the following indications: *1* is a water case; *2* is a magnetostriction transformer; *3* is an ultrasound concentrator; *4* is a sample of material under study in dense contact with the ultrasound concentrator; *5* is a vacuum furnace; a cryostat can be installed to perform low temperature tests; *6* a flange with current inputs; *7* are power supports; *8* are dynamometers with piezoprobes of force; *9* is a sylphon; *10* are worm reducing gears; *11* is a unit of a kinematic reducing array; *12* is a feed-screw; *13* is a dynamometer with piezoprobes of deformation; *14* is a diffusion pump.

– in atmosphere or under low vacuum conditions;
– under uniaxial tension or compression with the deformation rate range from 0.01 to 4 mm/min;
– within the temperature range from 77 to 1500 K;
– vibration amplitudes may vary from 0 to 12 microns.

The amplitude of ultrasonic vibrations (USV) is controlled with the UVM-4M vibrometre to the 0.1-micron accuracy.

Under mechanical tests performed, the USV amplitude was equal to 10 microns. Hence, the amplitude of cyclic stresses approached 275 MPa.

3. RESULTS

Figure 4 presents the data of standard, without USV, mechanical tests of nanocrystalline titanium under confined compression. The sample experiences strong deformation up to the value $e_{max} = 1.42$. Hence, the ratio of the sample diameter to its height changed from 0.63 to 2.3. The stress–strain curve (Fig. 4, *a*) demonstrates that yield defor-

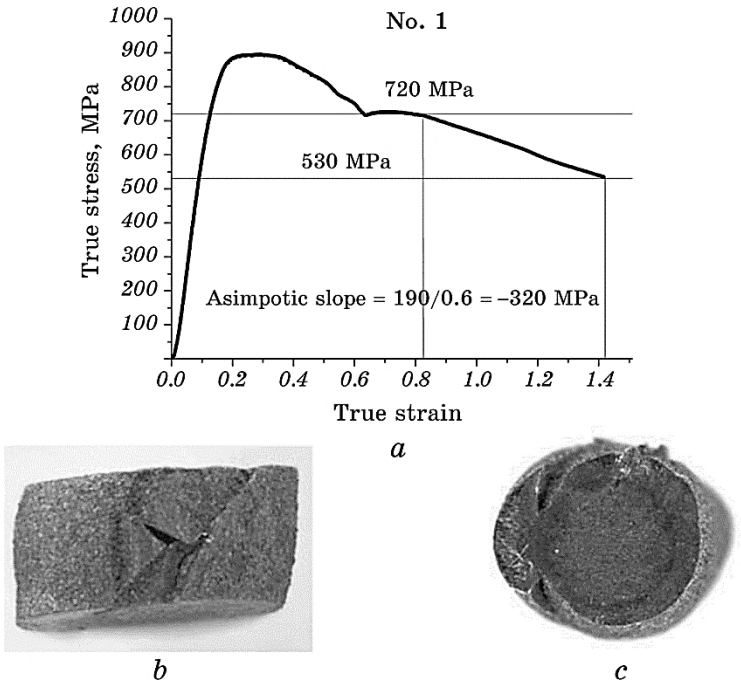

Fig. 4. Results of mechanical tests of nanocrystalline titanium on compression without USV for the initial strain rate of $\dot{\varepsilon} = 10^{-4}$ s^{-1}: true stress–true strain curve (*a*); optical image of the sample after tests, side view (*b*); the same sample viewed from above (*c*).

mation process starting at $\sigma > \sigma_{0.2} > 820$ MPa includes a short stage of dislocation hardening at which the stress value approaches maximum, $\sigma_{max} = 895$ MPa. After that, a softening stage follows caused by dislocation restructuring and shear band formation. Changes in the dislocation structure generate a smooth uniform decrease in stress, whereas the formation of shear bands manifests itself in wavy sections and a dip (at $e = 0.64$) on the stress–strain curve. Under large deformations (for $e > 1$), a linear section with a negative slope appears on the stress–strain curve. The slope value equals 320 MPa.

One readily observes the major shear band crossing the sample in the photos (Fig. 4, *b* and 4, *c*). One also observes the outcropping cracks and breaks in the place where the major shear band branches and its near-by exit on a butt-end surface. Barrel-shaped profile of the deformed sample is formed due to its uniform (dislocation) plastic deformation under confined compression. The profile curvature of the lateral surface is not constant because a sample fragmentation occurs during the shear banding generates non-uniform inner stresses and, correspondingly, non-uniform dislocation plastic deformation of the fragments. The absence of remarkable jump-like deformations for $e > 1$ indicates that secondary shear bands are formed in the region within the fragments divided earlier by the main shear band, whereas new shear bands crossing several fragments do not form. We did not study the set of secondary localized shear bands.

Results of mechanical tests of nanocrystalline titanium under the action of 10 microns amplitude (amplitude of cyclic stresses $\sigma \cong 275$ MPa) are presented in Fig. 5. USVs were switched on at the moment, when the uniform stress approached the magnitude of 100 MPa.

At this moment, the maximum stress (370 MPa) was substantially below the yield stress. Already the first seconds of the USV action affected the deformation curve considerably. The short-term material softening is changed into hardening. Then, at $e > 0.04$, scarce and shallow dips appear on the stress–strain curve. Finally, at $\sigma = 690$ MPa and $e = 0.11$, a jump-like sample de-loading occurred because of the major shear band formation shown in Fig. 5, *b*. To this moment, the uniform plastic deformation did not lead to a noticeable deformation of the profile as well as of the butt surface of the sample (Fig. 5, *c*), but the tip of the larger fragment is bulged-in under the action of the butt of USV concentrator. The sample fragments separated by the major shear band are shifted with respect to each other by the distance of 0.16 mm along the axis and they experienced an insignificant rotation around the axis. Thus, the remaining plastic strain due to this displacement amounts to 4%.

Note that the absence of remarkable barrel-shaped change of the lateral surface of the sample indicates the insignificance of the dislocation component of the plastic deformation before the major shear band

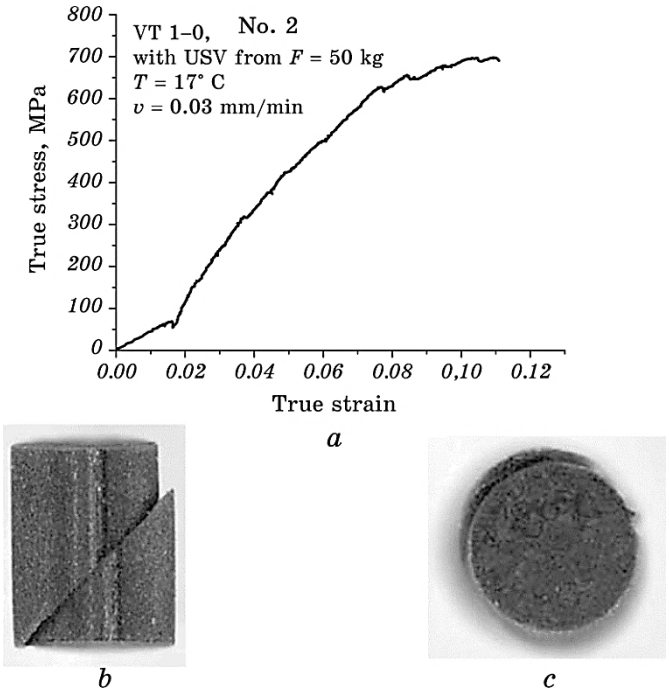

Fig. 5. Results of mechanical tests of nanocrystalline titanium on compression for the initial deformation rate of $\dot{\varepsilon} = 10^{-4}$ s^{-1}: true stress–true strain curve (*a*); optical image of the sample after tests, side view (*b*); the same sample viewed from above (*c*).

formation. This circumstance shows that the major shear band initiation occurred in the first place thanks to USV vibrations affecting the grain boundaries.

In order to clarify to what extent the impact of USV vibration depends on deformation rate, we performed mechanical tests increasing the deformation rate by an order of magnitude, up to the value $\dot{\varepsilon} = 10^{-4}$ s^{-1}. Figures 6 and 7 present the results of these tests.

In the stress–strain curve obtained under tests without USV (Fig. 6), a weak minimum is registered at $e = 0.43$ indicating the formation of the major shear band which edge on the surface may be observed in Fig. 6, *b* and *c*. The major shear band branches at the branching point and cracks have been formed at the butt surface. The shape of the lateral surface profile is barrel-like and (in contrast to what one observes in Fig. 5, *b* and *c*) the non-uniformity of its curvature is insignificant. One may conclude that the distribution of inner strains in the sample is weakly distorted by the major shear band development, and a formation process of new shear bands localized in the fragments separated by the major band is suppressed at the deformation rate chosen.

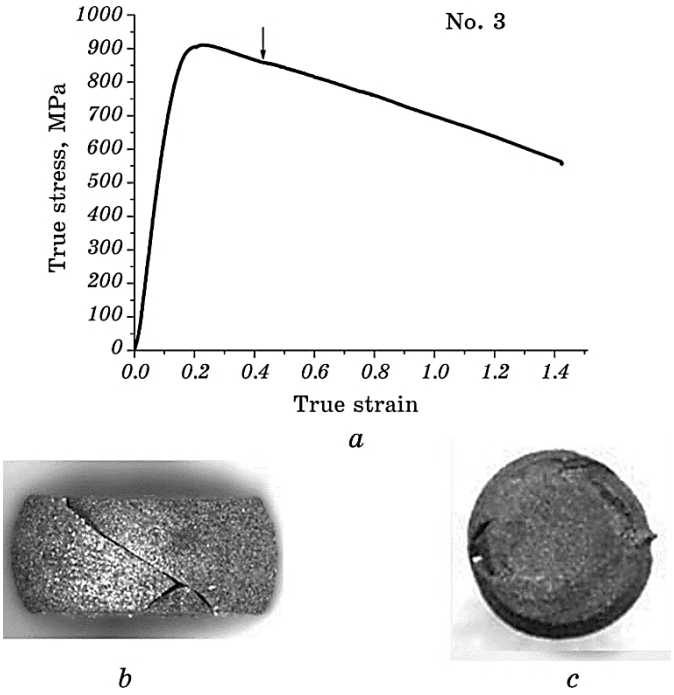

Fig. 6. Results of mechanical tests of nanocrystalline titanium on compression without vibrations with the initial deformation rate $\dot{\varepsilon} = 10^{-3}$ s^{-1}: true stress–true strain curve, the arrow marks the bend on the curve at $e = 0.43$ (*a*); optical image of the sample after tests, side view (*b*); the same sample viewed from above (*c*).

The negative slope of the rectilinear section of the stress–strain curve equals 290 MPa, what is 10% less in absolute value than the slope magnitude at $\dot{\varepsilon} = 10^{-4}$ s^{-1}. Taking into account the circumstance that there is no indication of intense formation of shear bands under large deformations in contrast to sample No. 1, we may conclude that the measured slope of the stress–strain curve is caused by the dislocation de-hardening.

Figure 7 shows the stress–strain curve in the presence of USV vibrations (strain rate $\dot{\varepsilon} = 10^{-3}$ s^{-1}) and the sample image after large deformation ($e = 1.5$). Appearance of multiple shear bands and the nonmonotonic pattern of the stress–strain curve caused by their formation at $e > 0.23$ (at the stage of sample softening), is visible. (Note that the stress–strain curve (Fig. 5, *a*) for the sample No. 2 tested under a slower quasi-static loading with superimposed USV (at $\dot{\varepsilon} = 10^{-4}$ s^{-1}) becomes nonmonotonic already under comparatively small stress and strain (for $e > 0.04$) at the stage of hardening.) In contrast to sample No. 3, the curvature of the lateral surface of sample No. 4 is substantially non-

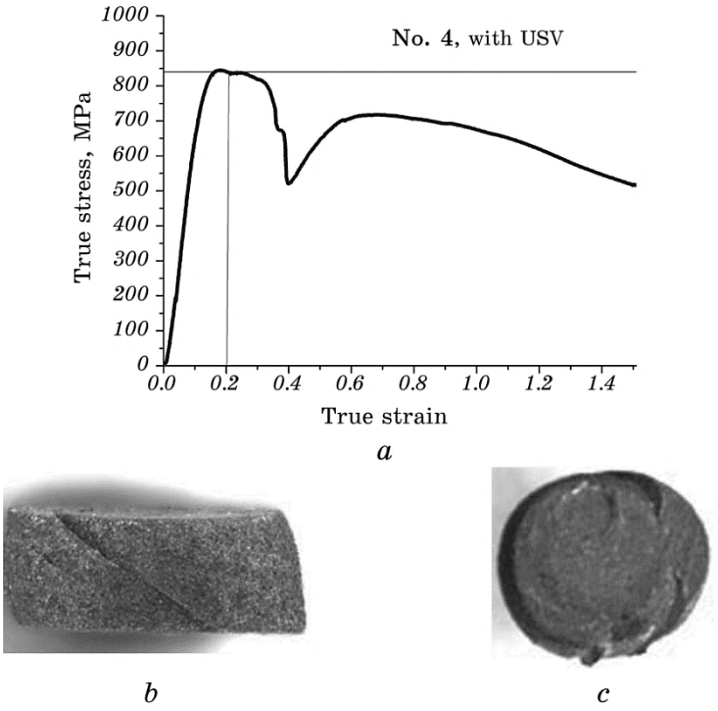

Fig. 7. Results of mechanical tests of nanocrystalline titanium on compression under ultrasound with the initial deformation rate $\dot{\varepsilon} = 10^{-3}$ s^{-1}: true stress–true strain curve (*a*); optical image of the sample after tests, side view (*b*); the same sample viewed from above (*c*).

uniform (Figs. 6, *b* and *c*). As was the case with sample No. 1, we think that this is the consequence of non-uniformity of inner strains appearing due to multiple slipping bands (one may observe some of them at the lateral and butt surfaces), breaking the uniformity of the sample dislocation flow.

The magnitude of the negative slope of the rectilinear section of the stress–strain curve under large deformations comprises 350 MPa, which is larger in absolute value than the negative slope of a similar rectilinear section of the stress–strain curve for sample No. 3. One would attribute more considerable softening of sample No. 4 to multiple shear bands formed in it.

4. DISCUSSION

The average grain size in titanium used in our experiments exceeds more than twice the characteristic size $d_c \cong 15$ nm on approaching which the change of the dominating mode of plastic deformation oc-

curs. Therefore, one regards the dislocation mechanism providing the macroscopically uniform flow of samples under uniform confined compression to be dominating for this material.

Paper [21] reports the data on standard mechanical compression tests of nanocrystalline Ni–W metal obtained by means of electrolytic deposition. Three batches of micron scale samples differed in average grain size: 5 nm, 15 nm, and 90 nm. The strain rate was equal to $\dot{\varepsilon} = 3.2 \cdot 10^{-4}\ s^{-1}$. This rate value is intermediate with respect to two strain rate values used in our experiments.

As was shown in [21], a uniform plastic deformation without formation of catastrophic localized shear bands with considerable deformation values $\cong 0.3$ occurs for the average grain size of 90 nm. The profile of the lateral sample surface is barrel-shaped. With smaller size of the grain, 5 nm and 15 nm, the plastic deformation of samples is non-uniform due to formation of catastrophic shear bands.

Results of our experiments performed without USV are well comparable with the data of paper [21]. One has to take into account that our samples possess millimetre-range size, and our material contains the grains of rather broad size distribution and its main part has dimensions within the 20–80 nm limits. Besides, quite large magnitudes of true strain about 1.4 were achieved in the course of tests, which data were presented here.

As one observes in Fig. 4, the formation of the major shear band occurred at $e = 0.64$ when the strain rate equalled $\dot{\varepsilon} = 10^{-4}\ s^{-1}$. At the deformation rate of $\dot{\varepsilon} = 10^{-3}\ s^{-1}$, the formation of the major shear band occurred at somewhat smaller strain value, $e = 0.43$.

Let us note that in experiments [21], with the grain size 90 nm of nanocrystalline Ni–W, the major shear band development was not achieved at the true strain $\cong 0.3$.

Substantially asymmetric profile of the lateral surface obtained at a slower deformation rate of $\dot{\varepsilon} = 10^{-4}\ s^{-1}$ (Fig. 4) points out to the non-uniform distribution of inner strains apparently appearing because of the inner shear banding, which causes the sample fragmentation and generates the non-uniform dislocation plastic deformation.

The revealed USV impact on mechanical properties of nanocrystalline titanium under uniaxial compression is accomplished through affecting the dislocation system as well as the grain boundaries. Apparently, the former as well as the latter ones introduce comparable contributions into the plastic deformation. As grain boundaries limit or impede dislocation slipping, both these mechanisms of USV affecting the hardness and yield of nanocrystalline metals are interconnected, thus making difficult the interpretation of experimental results. Such difficulties do not arise for coarse-grain titanium because the dislocation mechanism of the plastic deformation dominates due to rather low boundary density [19, 20]. As an example of connection between the

dislocation mechanism and grain-boundary effects in nanocrystalline titanium, let us consider the effect not yet studied in detail, which consists in nonmonotonic pattern of the stress–strain curve at the ultrasound switching on. It is revealed at the initial stage of the quasi-static loading that the average stress is about 10% of the yield stress (Fig. 8). After ultrasound switched on, a short-term stage of softening establishes for several seconds, after which the stage of hardening appears. The $d\sigma/de$ derivative experiences a 1.85 increase compared to the value registered without ultrasound. A similar effect but much less expressed takes place also at a faster uniform loading, $\dot{\varepsilon} = 10^{-3}\ s^{-1}$.

A similar but much less expressed effect is also observed at a faster uniform loading, $\dot{\varepsilon} = 10^{-3}\ s^{-1}$.

As one observes in Fig. 5, under the action of ultrasound the stress–strain curve becomes nonlinear and jump-like at $\sigma > \sigma_{0.2USV} = 350$ MPa $\cong$ $\cong 0.4\sigma_{0.2}$. When the average stress approaches the value of 720 MPa, a catastrophic shear band is formed. To this moment, the action of ultrasound is persisting 1000 seconds during which the stress performs $2 \cdot 10^7$ cycles.

Increasing the deformation rate to $\dot{\varepsilon} = 10^{-3}\ s^{-1}$ weaken the effects of ultrasound action, as is evident in Fig. 8. In particular, here, we have $\sigma > \sigma_{0.2USV} = 820$ MPa $\cong 0.9\sigma_{0.2}$, and the time to the catastrophic shear band formation (at $e = 0.42$) is approximately equal to 410 seconds during which $8.2 \cdot 10^6$ cycles are performed.

Judging from the stress–strain curve pattern (Fig. 7) at $\dot{\varepsilon} = 10^{-3}\ s^{-1}$, the initiation of slip bands by vibrations takes place on exceeding the value $\sigma_{0.2USV}$ by the stress as it also occurs under slower deformations. One may draw the conclusion that irreversible fatigue changes in the

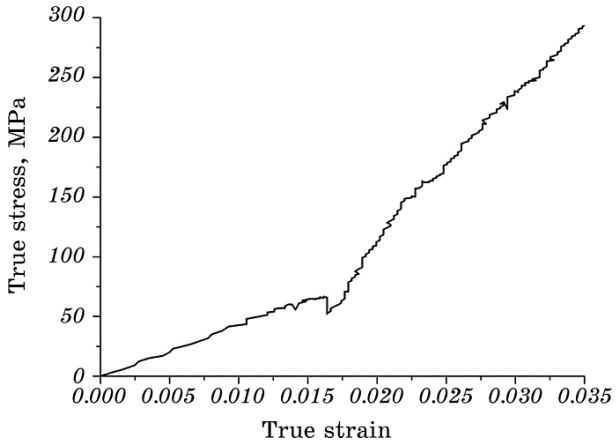

Fig. 8. Starting section of the stress–strain curve presented in Fig. 5. The stress–strain curve becomes nonlinear under ultrasound switched on. The arrow indicates the moment of the ultrasound switching on.

material structure and strength occur at the static stress exceeding the $\sigma_{0.2USV}$ value when the USV is superimposed.

5. CONCLUSIONS

In conclusion, our investigation outlined above shows that the ultrasonic cyclic stress acting on a dislocation system and grain boundaries produce accumulating irreversible structure changes which are slowed down or do not occur in a uniformly deformed material without the ultrasound. The reduction of the yield stress is one of the manifestations of these changes. The quantity $\sigma_{0.2USV}$ (it obviously depends on the initial structure state, the vibration intensity and the quasi-static deformation rate) is the mean stress exceeding which leads to the fast fatigue degradation of nanocrystalline titanium. The initiation of the major and secondary slip bands, reflected in the stress–strain curve pattern, displays the fatigue degradation under USV. This effect is enhanced with the deformation strain rate decreasing.

REFERENCES

1. C. C. Koch, I. A. Ovid'ko, S. Seal, and S. Veprek, *Structural Nanocrystalline Materials: Fundamentals and Applications* (Cambridge: Cambridge University Press: 2007).
2. K. S. Kumar, S. Suresh, M. F. Chisholm, J. A. Horton, and P. Wang, *Acta Mater.*, **51**: 87 (2003).
3. K. S. Kumar, H. Van Swygenhoven, and S. Suresh, *Acta Mater.*, **51**: 5743 (2003).
4. A. V. Sergueeva, N. A. Mara, and A. K. Mukherjee, *J. Mater. Sci.*, **42**: 1433 (2007).
5. Y. Estrin and A. Vinogradov, *Acta Mater.*, **61**: 782 (2013).
6. M. Dao, L. Lu, R. Asaro, J. Dehosson, and E. Ma, *Acta Mater.*, **55**: 4041 (2007).
7. M. A Meyers, A. Mishra, and D. J. Benson, *Prog. Mater. Sci.*, **51**: 427 (2006).
8. A. Vinogradov, *Mater. Sci. Forum*, 503–504: 267 (2006).
9. H. A. Padilla and B. L. Boyce, *Exp. Mech.*, **50**: 5 (2010).
10. R. A. Meirom, D. H. Alsem, A. L Romasco, T. Clark, R. G. Polcawich, J. S. Pulskamp, M. Dubey, R. O. Ritchie, and C. L. Muhlstein, *Acta Mater.*, **59**: 1141 (2011).
11. V. A. Filippenko, E. K. Sevidova, N. V. Dedukh, S. V. Malyshkina, A. A. Simonova, I. B. Timchenko, and V. A. Moskalenko, *Ortopediya, Travmotologiya i Protezirovanie*, **3**: 69 (2011) (in Russian).
12. A. V. Sergueeva, V. V. Stolyarov, R. Z. Valiev, and A. K. Mukherjee, *Scr. Mater.*, **45**: 747 (2001).
13. D. Jia, Y. M. Wang, K. T. Ramesh, E. Ma, Y. T. Zhu, and R. Z. Valiev, *Appl. Phys. Lett.*, 79: 611 (2001).
14. A. Vinogradov and S. Hashimoto, *Materials Transactions*, **42**: 74 (2001).
15. R. Z. Valiev, A.V. Sergueeva, and A. K. Mukherjee, *Scr. Mater.*, **49**: 669

(2003).
16. V. A. Moskalenko, A. R. Smirnov, and R. V. Smolyanets, *Fizika Nizkikh Temperatur*, **40**: 837 (2001) (in Russian).
17. A. V. Rusakova, S. V. Lubenets, L. S. Fomenko, and V. A. Moskalenko, *Fizika Nizkikh Temperatur*, **38**: 980 (2012) (in Russian).
18. V. A. Moskalenko, V. I. Betekhtin, B. K. Kardashev, A. G.Kadomtsev, A. R. Smirnov, R. V. Smolyanets, and M. V. Narykova, *Fizika Tverdogo Tela*, **56**: 1590 (2014) (in Russian).
19. M. Papakyriacoua, H. Mayer, C. Pypen, H. Plenk Jr., and S. Stanzl-Tschegg, *International Journal of Fatigue*, **22**: 873 (2000).
20. M. Papakyriacoua, H. Mayer, C. Pypen, H. Plenk Jr., and S. Stanzl-Tschegg, *Mater. Sci. Eng. A*, **308**: 143 (2001).
21. A. Khalajhedayati and T. J. Rupert, *Acta Mater.*, **65**: 326 (2014).
22. J. Schiøtz, T. Vegge, F. Di Tolla, and K. Jacobsen, *Phys. Rev. B*, **60**: 11971(1999).
23. A. S. Bakai, *Topics in Applied Physics*, **72**: 208 (1994).
24. A. S. Bakai, *Poliklasternye Amorfnye Tela* (Kharkov: Synteks: 2013) (in Russian).
25. N. P. Lazarev and A. S. Bakai, *J. Mech. Behav. Materials*, **22**: 119 (2013).
26. Yu. Petrusenko, A. Bakai, I. Neklyudov, S. Bakai, V. Borysenko, G. Wang, P. K. Liaw, L. Huang, and T. Zhang, *J. Alloys Compd.*, **509**: 123 (2011).
27. A. S. Bakai, S. A. Bakai, V. M. Gorbatenko, M. B. Lazarev, Yu. A. Petrusenko, and A. A. Scheretsky, *Nanorozmirni Systemy: Struktura, Vlastyvosti, Tekhnologiya. Doslidzhennya v Ukrayini* [Nanoscale Systems: Structure, Properties, Technology. Investigations in Ukraine] (Ed. A. G. Naumovets) (Kiev: Akademperiodika: 2014) (in Russian).
28. A. S. Bakai, S. A. Bakai, G. N. Malik, V. M. Gorbatenko, V. M. Netesov, V. A. Emlyaninov, *Problemy Atomnoy Nauki i Tekhniki. Seriya Radiatsionnaya Fizika i Radiatsionnoe Materialovedenie*, Iss. 4 (87): 104 (2005) (in Russian).
29. A. S. Bakai, V. V. Kul'ko, I. M. Mikhailovskij, V. B. Rabukhin, and O. A. Velikodnaja, *J. Non-Cryst. Solids*, **182**: 315 (1995).
30. A. S. Bakai, E. V. Sadanov, V. A. Ksenofontov, S. A. Bakai, J. A. Gordienko, and I. M. Mikhailovskij, *Metals*, **2**: 441 (2012).
31. I. M. Lifshitz, *ZhETF*, **17**: 909 (1963) (in Russian).
32. L. A. Greer, Y. Q. Cheng, and E. Ma, *Mater. Sci., Eng. R*, **74**: 71 (2013).
33. O. Bakai, *Physics of Liquid Matter: Modern Problems. Springer Proceedings in Physics* (Eds. L. Bulavin and N. Lebovka), vol. **171**, Ch. 5, p. 103 (2015).